

Theoretical Spectroscopic Study of the Conjugate Microcystin-LR-Europium Cryptate

Júlio G. Santos,^a José Diogo L. Dutra,^a Severino Alves Junior,^b Gilberto F. de Sá,^b
Nivan B. da Costa Junior^a and Ricardo O. Freire^{*,a}

^aDepartamento de Química, Universidade Federal de Sergipe,
49100-000 São Cristóvão-SE, Brazil

^bDepartamento de Química Fundamental, Universidade Federal de Pernambuco,
50590-470 Recife-PE, Brazil

Neste trabalho, ferramentas teóricas foram utilizadas no estudo de propriedades espectroscópicas do conjugado microcistina-LR-criptato de európio. O modelo Sparkle/AM1 foi aplicado na previsão da geometria do sistema e o modelo INDO/S-CIS foi utilizado no cálculo das energias dos estados excitados. Os parâmetros de Intensidade foram previstos baseados na teoria Judd-Ofelt e o modelo teórico baseado na teoria das transições 4f-4f foi aplicado no cálculo das taxas de transferência e de retrotransferência de energia, taxas de decaimento radiativo e não radiativo, eficiência e rendimento quânticos. Um estudo detalhado das propriedades luminescentes do conjugado microcistina-LR-criptato de európio foi realizado. Os resultados mostram que o rendimento quântico teórico de 23% está em bom acordo com valores experimentais publicados. Este fato sugere que este protocolo teórico pode ser usado para a concepção de novos sistemas objetivando melhorar as propriedades luminescentes. Os resultados sugerem que este sistema luminescente pode ser um bom conjugado para ser usado no teste ELISA para detecção por fluorescência da microcistina-LR em água.

In this work, theoretical tools were used to study spectroscopic properties of the conjugate microcystin-LR-europium cryptate. The Sparkle/AM1 model was applied to predict the geometry of the system and the INDO/S-CIS model was used to calculate the excited state energies. Based on the Judd-Ofelt theory, the intensity parameters were predicted and a theoretical model based on the theory of the 4f-4f transitions was applied to calculate energy transfer and backtransfer rates, radiative and non-radiative decay rates, quantum efficiency and quantum yield. A detailed study of the luminescent properties of the conjugate Microcystin-LR-europium cryptate was carried out. The results show that the theoretical quantum yield of luminescence of 23% is in good agreement with the experimental value published. This fact suggests that this theoretical protocol can be used to design new systems in order to improve their luminescence properties. The results suggest that this luminescent system may be a good conjugate for using in assay ELISA for detection by luminescence of the Microcystin-LR in water.

Keywords: theoretical prediction, luminescence, Sparkle Model keyword, supramolecular compounds

Introduction

The research involving luminescent lanthanide systems has grown since the late 80.¹ The search of luminescent lanthanide complexes has been substituted by the study of interesting systems known as metal-organic frameworks (MOF).²⁻⁴ However, the interest in lanthanide cryptates still remains.⁵⁻⁷ This fact can be explained by the possibility

of the potential use of such complexes as luminescent materials, chemical probes and new sensors for biological applications.⁸

This kind of ligand can encapsulate the lanthanide ion preventing the coordination of molecules having CH, NH or OH bonds. This avoids the quenching of the luminescence due nonradiative deactivation via the C-H, N-H or O-H vibrations.⁹ Figure 1 shows an example of cryptate ligand. It can be observed in Figure 1a that the lanthanide ion was inside of the ligand, well protected from the solvent

*e-mail: rfreire@ufs.br

molecules. Figure 1b gives us an idea of the size of this cavity. In this cryptate, for example, it is possible insert a sphere with a radius of 2.3 Å.

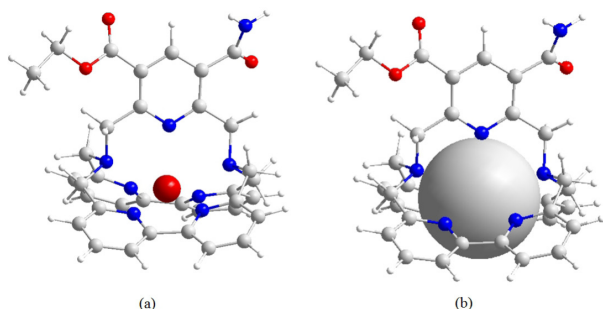


Figure 1. Structure of the representative cryptate complex.

In order to become useful this kind of complex as label of biological molecules, the cryptate must have a reactive group for attachment of a biomolecule. In the complex shown in Figure 1, this group linked to pyridine group can be observed. The formation of macromolecular adducts between a lanthanide complex and a biomolecule such as a protein or enzyme could be reached via the formation of either covalent or noncovalent interactions.

In 2004, Vila-Nova *et al.*¹⁰ published the synthesis, characterization and experimental study of the spectroscopic properties of lanthanide cryptates $[\text{Ln}(\text{bipy})_2\text{py}(\text{CO}_2\text{Et})_2]^{3+}$ with $\text{Ln} = \text{Eu}^{3+}$, Tb^{3+} or Gd^{3+} . In this work, the authors observed in solution a quantum yield of luminescence of 25 and 14% for the systems with Tb^{3+} and Eu^{3+} , respectively. They concluded that the better resonance between the ligand triplet state and the Tb^{3+} excited levels can justify the luminescence of the systems. Moreover, they carried out with the theoretical study of the $[\text{Eu}(\text{bipy})_2\text{py}(\text{CO}_2\text{Et})_2]^{3+}$ that presented a theoretical quantum yield of 19%.

Based on this results, two years later, a new work was published and Vila-Nova *et al.*⁸ proposed a fluorescent-labeled microcystin-LR $[\text{Tb}(\text{bipy})_2\text{py}(\text{CO}_2\text{Et})_2]^{3+}$ cryptate. This work was motivated by a tragic accident that happened in the Caruaru City in the Northeast of Brazil in 1996. At that time, 76 of a total of 131 patients died during a haemodialysis treatment. This accident happened because the water used in the procedure was contaminated with microcystin. This cyanobacterium is very resistant to high temperatures, and when it is present in the water, keeps the toxicity even after boiling. In humans, the microcystins can lead to a higher incidence of liver cancer.¹¹ However, it has a more potent action when applied directly into the bloodstream than when ingested, explaining the large number of deaths in Caruaru City. As result of this work, Vila-Nova *et al.*⁸ obtained the conjugate Microcystin-LR-terbium cryptate and the spectroscopic study showed that the system is luminescent.

To use the assay ELISA for detection of Microcystin-LR in water by luminescence, the luminescent cryptate must be linked to Microcystin-LR. The concentration of the cyanobacteria is determined by a correlation with the observed luminescence. Thereby, it is fundamental that the cryptates present luminescence in solution. The conjugate obtained by Vila-Nova *et al.*⁸ is not appropriated because it displays low luminescence intensity after the conjugation.

In this work, our group used theoretical tools for the study of the luminescent properties of the conjugate Microcystin-LR-europium cryptate aiming to understand details involved in the luminescent process. This detailed comprehension, hereafter, can be used to design new systems with high luminescence, more appropriated for application in assay ELISA.

Methodology

The ground state geometry of the conjugate microcystin-LR-europium cryptate was calculated using the Sparkle/AM1 model,¹²⁻¹⁴ implemented in the Mopac 2009 package.¹⁵ The keywords used in the calculation reported in this work were: AM1, PRECISE, BFGS, GNORM = 0.25, SCFCRT = 1.D-10 (to increase the SCF (self consistent field) convergence criterion) and XYZ (for cartesian coordinates). The Sparkle/PM3¹⁶ and Sparkle/PM6¹⁷ models were also applied and showed similar results to those obtained with the Sparkle/AM1 model.

The Sparkle/AM1 optimized geometry was used to calculate the singlet and triplet excited states using configuration interaction single (CIS) based on the intermediate neglect of differential overlap/spectroscopic (INDO/S) technique^{18,19} implemented in ZINDO program.²⁰

The intensity parameters Ω_λ ($\lambda = 2, 4$ and 6) were calculated using the Judd-Ofel't theory^{21,22} after which the Ω_λ parameters are defined by:

$$\Omega_\lambda = (2\lambda + 1) \sum_{t,p} \frac{|B_{\lambda tp}|^2}{(2t + 1)} \quad (1)$$

with

$$B_{\lambda tp} = \frac{2}{\Delta E} \langle r^{t+1} \rangle \theta(t, p) \gamma'_p - \left[\frac{(\lambda + 1)(2\lambda + 3)}{2\lambda + 1} \right] \langle r^t \rangle (1 - \sigma_\lambda) \langle f \| C^{(\lambda)} \| f \rangle \Gamma'_p \delta_{t,\lambda+1} \quad (2)$$

The $B_{\lambda tp}$ parameter consists of the sum of two terms: the first term contributes positively and refers only to the forced electric dipole component whereas the second term contributes negatively and refers only to the dynamic coupling component. Details on the parameters of equations 1 and 2 are widely discussed in the literature.²³⁻²⁵

The calculated intensity parameters associated with the singlet and triplet energies and R_L values were used to

calculate the energy transfer and backtransfer rates. The R_L values were calculated by:

$$R_L = \frac{\sum_i c_i^2 R_{L,i}}{\sum_i c_i^2} \quad (3)$$

with c_i being the molecular orbital coefficient of the atom i contributing to the ligand state (triplet or singlet) involved in the energy transfer, and $R_{L,i}$ corresponding to the distance from atom i to the Eu^{3+} ion.

The energy transfer rates are obtained by the sum of two terms: W_{ET}^{em} obtained from the exchange mechanism and W_{ET}^{mm} obtained from the multipolar mechanism. These terms were calculated by:

$$W_{ET}^{em} = \frac{8\pi}{3h} \frac{e^2(1-\sigma_0)^2}{(2J+1)R_L^4} F \langle \alpha'J' \| S \| \alpha J \rangle^2 \sum_m \left| \langle \phi | \sum_k \mu_z(k) s_m(k) | \phi' \rangle \right|^2 \quad (4)$$

and

$$W_{ET}^{mm} = \frac{2\pi}{h} \frac{e^2 S_L}{(2J+1)G} F \sum_\lambda \gamma_\lambda \langle \alpha'J' \| U^{(\lambda)} \| \alpha J \rangle^2 + \frac{2\pi}{h} \frac{e^2 S_L}{(2J+1)G R_L^6} F \sum_\lambda \Omega_\lambda^{ed} \langle \alpha'J' \| U^{(\lambda)} \| \alpha J \rangle^2 \quad (5)$$

where S is the total spin operator of the lanthanide ion, μ_z is the z component of the electric dipole operator and s_m ($m=0, \pm 1$) is a spherical component of the spin operator (both for the ligand electrons), and σ_0 is a distance-dependent screening factor. G is the degeneracy of the ligand initial state and a specifies a given 4f spectroscopic term, J is the total angular momentum quantum number of the lanthanide ion.

The quantity F corresponds to the factor dependent of the temperature, and contains a sum about the Frank Condon's factors, given by:

$$F = \frac{1}{h\gamma_L} \sqrt{\frac{\ln 2}{\pi}} \exp \left[- \left(\frac{\Delta}{h\gamma_L} \right)^2 \ln 2 \right] \quad (6)$$

where γ_L is the ligand state band width-at-half-maximum, and Δ is the transition energy difference between the donor and acceptor involved in the transfer process.

$$\gamma_\lambda = (\lambda + 1) \frac{\langle r^\lambda \rangle^2}{(R_L^{\lambda+2})^2} \langle 3 \| C^{(\lambda)} \| 3 \rangle^2 (1 - \sigma_\lambda)^2 \quad (7)$$

The theoretical quantum yield of the 5D_0 level is given by:

$$q = \frac{\eta(^5D_0)}{\Phi \eta(S_0) \tau_r(^5D_0)} \quad (8)$$

where $\frac{1}{\tau_r(^5D_0)}$ is the total radiative decay rate from the

5D_0 level. The appropriate set of rate equations is:

$$\frac{d\eta(S_1)}{dt} = - \left(\frac{1}{\tau(S_1)} \eta(S_1) + W_{ET} \eta(^5D_4) \right) + (\Phi \eta(S_0) + W_{BT} \eta(^5D_4)) \quad (9)$$

$$\frac{d\eta(T)}{dt} = - \left(W_{ET} \eta(^5D_4) + W_{ET} \eta(^5D_0) + \frac{1}{\tau(T)} \right) \eta(T) + (\Phi \eta(S_1) + W_{BT} \eta(^5D_4) + W_{BT} \eta(^5D_0)) \quad (10)$$

$$\frac{d\eta(^5D_4)}{dt} = - (W_{BT1} + k_1) \eta(^5D_4) + W_{ET} \eta(S_1) \quad (11)$$

$$\frac{d\eta(^5D_1)}{dt} = - (W_{BT2} + k_2) \eta(^5D_1) + (k_1 \eta(^5D_4) + W_{ET} \eta(T)) \quad (12)$$

$$\frac{d\eta(^5D_0)}{dt} = - (A_{rad} + A_{nr} + W_{BT3}) \eta(^5D_0) + (k_2 \eta(^5D_1) + W_{ET} \eta(T)) \quad (13)$$

$$\eta(^5D_4) + \eta(^5D_1) + \eta(^5D_0) + \eta(^7F_0) = 1 \quad (14)$$

$$\eta(S_0) + \eta(T) + \eta(S_1) = 1 \quad (15)$$

Results and Discussions

Figure 2 shows the optimized ground state geometry of this structure. It is possible to assume that the europium cryptate was linked to microcystin-LR by a small spacer. The coordination polyhedron of the europium cryptate is formed by seven nitrogen atoms of the polydentate ligand (Figure 1b) and one oxygen atom from the water molecule.

Table 1 presents the intensity parameters Ω_λ ($\lambda = 2, 4$ and 6), radiative (A_{rad}) and non-radiative (A_{nr}) decay rates, quantum efficiency (η) and quantum yield (q) values calculated for $[\text{Eu}(\text{C}(\text{bipy})_2\text{py}(\text{CO}_2\text{Et})_2)]^{3+}$ cryptate and for the conjugate microcystin-LR-europium cryptate. The results obtained for $[\text{Eu}(\text{C}(\text{bipy})_2\text{py}(\text{CO}_2\text{Et})_2)]^{3+}$ cryptate agree perfectly with the results published by Vila-Nova *et al.*¹⁰ In the analysis of the results calculated for the conjugate microcystin-LR-europium cryptate, the small values of the Ω_2 and Ω_4 parameters suggest the occurrence of a chemical environment weakly polarizable and rigid surrounding the europium trivalent ion. This observation is consistent with the nature of the macrocyclic ligand coordinated to the europium ion. The A_{rad} decay rate is approximately 1/3 of the A_{nr} decay rate. This fact justifies the quantum yield of about 23%.

The ideal energy transfer condition occurs when the excited state of the ligand is about 1500 cm^{-1} above of the europium excited state. As can be observed in Table 2, the singlet excited state is about 3000 cm^{-1} above 5D_4 level. This fact explains the small $S \rightarrow ^5D_4$ energy transfer rate ($5.7 \times 10^5 \text{ s}^{-1}$). Taking attention to the excited triplet energy of the ligand, the differences considering 5D_1 and 5D_0 excited levels are 8366 and 10100 cm^{-1} respectively. However, it is possible to assume that the $T \rightarrow ^5D_1$ and $T \rightarrow ^5D_0$ energy transfer rates are greater than the $S \rightarrow ^5D_4$ energy transfer rate. This can be explained because

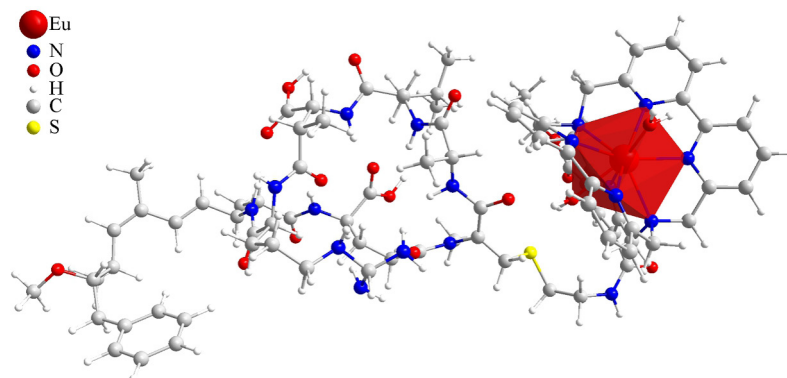


Figure 2. The ground state geometry of the conjugate microcystin-LR-europium cryptate calculated using the semiempirical Sparkle/AM1 model.¹³

Table 1. Theoretical intensity parameters Ω_2 , Ω_4 and Ω_6 , radiative (A_{rad}) and non-radiative (A_{nrad}) decay rates, quantum efficiency (η) and quantum yield (q) values

	Intensity parameters / 10^{-20} cm^2			A_{rad} / s^{-1}	A_{nrad} / s^{-1}	$\eta / \%$	$q / \%$
	Ω_2	Ω_4	Ω_6				
$[\text{Eu}(\text{bipy})_2\text{py}(\text{CO}_2\text{Et})_2]^{3+}$	3.96	5.34	0.07	250.7	1046.5	19.3	19.1
Microcystin-LR + $[\text{Eu}(\text{bipy})_2\text{py}(\text{CO}_2\text{Et})_2]^{3+}$	5.92	4.70	0.06	299.8	998.9	23.1	22.9

for the $^5\text{D}_0$ and $^5\text{D}_1$ levels, the exchange mechanism dominates, whereas for the $^5\text{D}_4$ levels, the dipole-dipole mechanism is the most important one. At first, the energy transfer between the triplet and $^5\text{D}_0$ is forbidden for both mechanisms, but this selection rule can be relaxed due to the thermal population of the $^7\text{F}_1$ level at room temperature and via the mixing of the J states due to the interaction with the ligand field.

In Figure 3, it is presented an energy level diagram showing the most probable channel for the intramolecular energy transfer process. Full lines concern the radiative transitions, whereas the dashed lines concern those associated with non-radiative paths. The curved lines are related to the ligand \rightarrow lanthanide energy transfer or backtransfer. Typical values of the remaining transfer rates were assumed to be identical to those found for coordination compounds, namely $\Phi = 10^4$, $\Phi(1) = 10^8$, $1/\tau(\text{S}_1) = 10^6$ and $1/\tau(\text{T}) = 10^5 \text{ s}^{-1}$.²⁶ The energy transfer rates from the ligand singlet state (S_1) to the $^5\text{D}_4$ level and from the ligand triplet state (T_1) to the $^5\text{D}_1$ and $^5\text{D}_0$ levels are summarized in Table 2.

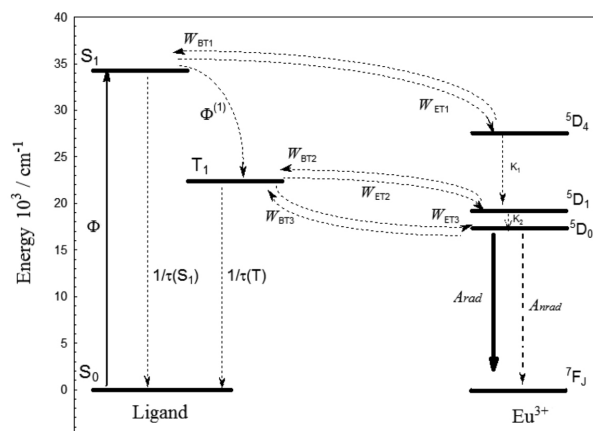


Figure 3. Energy level diagram for the conjugate microcystin-LR-europium cryptate showing the most probable channels for the intramolecular energy transfer process.

Conclusions

In the present work, it was carried out a theoretical spectroscopic study of the conjugate microcystin-LR-

Table 2. Calculated values of intramolecular energy transfer and backtransfer rates for microcystin-LR-europium cryptate

Structure	Ligand state / cm^{-1}	\rightarrow	4f state / cm^{-1}	$R_L / \text{\AA}$	Transfer rate / s^{-1}	Backtransfer rate / s^{-1}
Sparkle/AM1	singlet (30522.7)	\rightarrow	$^5\text{D}_4$ (27586)	3.97	$W_{\text{ET1}} = 5.7 \times 10^5$	$W_{\text{BT1}} = 4.5 \times 10^{-1}$
	triplet (27392.8)	\rightarrow	$^5\text{D}_1$ (19027)	5.18	$W_{\text{ET2}} = 1.5 \times 10^8$	$W_{\text{BT2}} = 6.2 \times 10^{-10}$
	triplet (27392.8)	\rightarrow	$^5\text{D}_0$ (17293)	5.18	$W_{\text{ET3}} = 3.3 \times 10^7$	$W_{\text{BT3}} = 2.8 \times 10^{-14}$

europium cryptate. All luminescent properties were calculated using well-established models. The results suggest a quantum yield of luminescence of about 23% for the europium cryptate when conjugate to microcystin-LR protein. The results show that the predicted parameter is in a good agreement with the experimental data. This suggests that the theoretical protocol applied here can be used to design new systems in order to improve their luminescence properties. This luminescent system may be a good conjugate to be used in the ELISA assay for detection by luminescence of the microcystin-LR in water.

Acknowledgments

We appreciate the financial support from the Brazilian agencies, institutes and networks: CNPq, CAPES, FAPITEC-SE, INAMI and RENAMI. The authors also thank Dra. Iara de Fátima Gimenez for the revision of the text.

References

1. de Sá, G. F.; Malta, O. L.; de Mello Donegá, C.; Simas, A. M.; Longo, R. L.; Santa-Cruz, P. A.; da Silva Jr., E. F.; *Coord. Chem. Rev.* **2000**, *196*, 165.
2. Carlos, L. D.; Almeida Paz, F. A.; Ananias, D.; *Chem. Soc. Rev.* **2011**, *40*, 926.
3. Weber, I. T.; Terra, I. A. A.; Melo, A. J. G. D.; Lucena, M. A. D. M.; Wanderley, K. A.; Paiva-Santos, C. O.; Antônio, S. G.; Nunes, L. A. O.; Paz, F. A. A.; de Sá, G. F.; Júnior, S. A.; Rodrigues, M. O.; *RSC Advances* **2012**, *2*, 3083.
4. Rodrigues, M. O.; Paz, F. A.; Freire, R. O.; de Sa, G. F.; Galembeck, A.; Montenegro, M. C.; Araujo, A. N.; Alves, S.; *J. Phys. Chem. B* **2009**, *113*, 12181.
5. Alzakhem, N.; Bischof, C.; Seitz, M.; *Inorg. Chem.* **2012**, *51*, 9343.
6. Santos, J. G.; Dutra, J. D. L.; Alves Jr., S.; Freire, R. O.; da Costa Jr., N. B.; *J. Phys. Chem. A* **2012**, *116*, 4318.
7. Ohtsu, H.; Suzuki, T.; Ohtsuka, H.; Ishii, A.; Hasegawa M.; *Monatsh. Chem.* **2009**, *140*, 783.
8. Oliveira, E. J. A.; Vila Nova, S. P.; Alves Jr., S.; Santa-Cruz, P.; Molica, R. J. R.; Teixeira, A.; Malageño, E.; Filho, J. L. L.; *J. Braz. Chem. Soc.* **2006**, *17*, 243.
9. Bischof, C.; Wahsner, J.; Scholten, J.; Trosien, S.; Seitz, M.; *J. Am. Chem. Soc.* **2010**, *132*, 14334.
10. Vila-Nova, S. P.; Pereira, G. A. L.; Albuquerque, R. Q.; Mathis, G.; Bazin, H.; Autiero, H.; de Sá, G. F.; Alves Jr., S.; *J. Lumin.* **2004**, *109*, 173.
11. Chorus, I.; Bartram, J.; *Toxic Cyanobacteria in Water: A Guide to their Public Health Consequences, Monitoring and Management*; E & FN Spon: London, 1999, p.416.
12. de Andrade, A. V. M.; da Costa, Jr., N. B.; Simas, A. M.; de Sá, G. F.; *Chem. Phys. Lett.* **1994**, *227*, 349.
13. Freire, R. O.; Rocha, G. B.; Simas, A. M.; *Inorg. Chem.* **2005**, *44*, 3299.
14. Freire, R. O.; Costa Jr., N. B.; Rocha, G. B.; Simas, A. M. J.; *Chem. Theory and Comput.* **2006**, *2*, 64.
15. Stewart, J. J. P.; *MOPAC 2009*, Stewart Computational Chemistry: Colorado Springs, USA, 2009.
16. Freire, R. O.; Rocha, G. B.; Simas, A. M.; *J. Braz. Chem. Soc.* **2009**, *20*, 1638.
17. Freire R. O. and Simas, A. M.; *J Chem Theory and Comput.* **2010**, *6*, 2019.
18. Ridley, J. E.; Zerner, M. C.; *Theor. Chim. Acta* **1976**, *42*, 223.
19. Zerner, M. C.; Loew, G. H.; Kirchner, R. F.; Mueller-Westerhoff, U. T.; *J. Am. Chem. Soc.* **1980**, *102*, 589.
20. Zerner, M. C.; *ZINDO Manual QTP*; University of Florida: Gainesville, USA, 1990.
21. Judd, B. R.; *Phys. Rev.* **1962**, *127*, 750.
22. Ofelt, G.S.; *J. Chem. Phys.* **1962**, *37*, 511.
23. Malta, O. L.; Ribeiro, S. J. L.; Faucher, M.; Porcher, P.; *J. Phys. Chem. Solids* **1991**, *52*, 587.
24. Malta, O. L.; Couto dos Santos, M. A.; Thompson, L. C.; Ito, N. K.; *J. Lumin.* **1996**, *69*, 77.
25. Malta, O. L.; Brito, H. F.; Meneses, J. F. S.; Silva, F. R. G.; Alves Jr., S.; Farias Jr., F. S.; de Andrade, A. V. M.; *J. Lumin.* **1997**, *75*, 255.
26. Malta, O. L.; e Silva, F. R. G.; Longo, R.; *Chem. Phys. Lett.* **1999**, *307*, 518.

Submitted: November 15, 2012

Published online: January 22, 2013